Regulation of Desmosome Assembly in MDCK Epithelial Cells: Coordination of Membrane Core and Cytoplasmic Plaque Domain Assembly at the Plasma Membrane

Manijeh Pasdar,* Kathleen A. Krzeminski,‡ and W. James Nelson

Institute for Cancer Research, Philadelphia, Pennsylvania 19111

Abstract. Desmosomes are major components of the intercellular junctional complex in epithelia. They consist of at least eight different cytoplasmic and integral membrane proteins that are organized into two biochemically and structurally distinct domains: the cytoplasmic plaque and membrane core. We showed previously that in MDCK epithelial cells major components of the cytoplasmic plaque (desmoplakin I and II; DPI/II) and membrane core domains (desmoglein I; DGI) initially enter a pool of proteins that is soluble in buffers containing Triton X-100, and then titrate into an insoluble pool before their arrival at the plasma membrane (Pasdar, M., and W. J. Nelson. 1988. *J. Cell Biol.* 106:677–685; Pasdar, M., and W. J. Nelson. 1989. *J. Cell Biol.* 109:163–177). We have now examined whether either the soluble or insoluble pool of these proteins represents an intracellular site for assembly and interactions between the domains before their assembly into desmosomes at the plasma membrane. Interactions between the Triton X-100-soluble pools of DPI/II and DGI were analyzed by sedimentation of extracted proteins in sucrose gradients. Results show distinct differences in the sedimentation profiles of these proteins, suggesting that they are not associated in the Triton X-100-soluble pool of proteins; this was also supported by the observation that DGI and DPI/II could not be coimmunoprecipitated in a complex with each other from sucrose gradient fractions. Immunofluorescence analysis of the insoluble pools of DPI/II and DGI, in cells in which desmosome assembly had been synchronized, showed distinct differences in the spatial distributions of these proteins. Furthermore, DPI/II and DGI were found to be associated with different elements of cytoskeleton; DPI/II were located along cytokeratin intermediate filaments, whereas DGI appeared to be associated with microtubules. The regulatory role of cytoskeletal elements in the intracellular organization and assembly of the cytoplasmic plaque and membrane core domains, and their integration into desmosomes on the plasma membrane is discussed.

THE epithelial junctional complex comprises five major components: zonula occludens (24, 37), zonula adherens (14, 41), Ca^{2+}-dependent cell adhesion proteins (10, 16, 17, 18), gap junctions and desmosomes (6–8, 11, 13, 18, 22, 23). The coordinated assembly of these components at the plasma membrane, and their roles in maintaining cell–cell adhesion are important in the morphogenesis of tissues and organs in development and subsequent function of fully differentiated cells (39).

Of these components of the junctional complex, the desmosome has been extensively analyzed in terms of its protein composition and morphology. Desmosomes consist of at least eight different proteins that are organized into two biochemically, structurally and functionally distinct domains: a membrane core domain, which may be involved in intercellular adhesion (8), and a cytoplasmic plaque domain, which is the anchorage site for cytokeratin intermediate filaments and is attached to the membrane core domain. The membrane core domain consists of membrane glycoproteins (M_r 150,000 desmoglein I [DGI], 120,000/110,000 [desmocollin II/III], and 22,000). The cytoplasmic plaque is composed of non-glycosylated proteins (the desmoplakins [DP][1]; M_r 250,000 [DPI], 215,000 [DPII], 83,000 [DPIII, also called plakoglobin] and 78,000 [DPIV]). Given the complexity of proteins that make up the desmosome, the question arises as to how assembly of these two domains is coordinated during cell–cell interactions.

Early morphological studies demonstrated that desmosomes are assembled rapidly on the plasma membrane of adjacent epithelial cells upon induction of cell–cell contact (30). Significantly, assembly appeared to occur from preex-

M. Pasdar's present address is Department of Anatomy and Cell Biology, Faculty of Medicine, University of Alberta, Edmonton, Alberta, Canada. W. J. Nelson's present address is Department of Molecular and Cellular Physiology, Stanford University School of Medicine, Stanford, CA 94305-5426.

1. *Abbreviations used in this paper*: DG, desmoglein; DP, desmoplakin.

isting pools of proteins in the cytoplasm and on the plasma membrane. Subsequent biochemical analyses provided insight into the nature of these preexisting pools of desmosomal proteins. Studies (31, 32) of DPI/II, two major proteins of the cytoplasmic plaque domain, showed that these proteins initially form a soluble ~7.3S protein complex that is readily extracted from cells with buffers containing Triton X-100. The DPI/II complex is subsequently transferred to an insoluble pool that is not extractable from the cell with buffers containing high salt and Triton X-100. The formation of these two pools of DPI/II occurs independently of cell-cell contact, but in the absence of cell-cell contact both pools are degraded rapidly ($t_{1/2}$ ~8–10 h). Upon induction of cell-cell contact, however, ~75% of the DPI/II complex is transferred from the soluble to the insoluble pool and is stabilized in the form of an assembled desmosome at the plasma membrane. A comparable analysis (33) of the steps involved in the assembly of DGI, a major protein of the membrane core domain showed that DGI was also present initially in a soluble pool of proteins. However, after oligosaccharide processing, the soluble pool of DGI was transferred into an insoluble pool in the Golgi complex, and then transported to the plasma membrane. In the absence of cell-cell contact DGI was degraded rapidly ($t_{1/2}$ ~4 h), but after cell-cell adhesion DGI became metabolically stable in the form of an assembled desmosome.

That desmosomes rapidly assemble (within minutes) from these preexisting pools of proteins raises the possibility that interactions between proteins of different domains may occur intracellularly before formation of desmosomes at the plasma membrane. Such an interaction would provide a simple mechanism for regulating the assembly of these desmosomal domains into a single structure at the plasma membrane. Consequently, we have searched in the present study for intracellular interactions between representative components of the cytoplasmic plaque (DPI/II) and membrane core (DGI) domains. The results indicate that DPI/II and DGI do not interact intracellularly before desmosome assembly. Furthermore, we show that these proteins are associated with different cytoskeletal filaments in the cytoplasm before desmosome assembly at the plasma membrane. These results indicate that interactions between the cytoplasmic plaque and membrane core domains are probably initiated at the plasma membrane, and that different cytoskeletal elements regulate the intracellular organization and transfer of protein components of these domains to the plasma membrane prior to desmosome assembly.

Materials and Methods

Cells

The culture conditions used to grow MDCK cells have been described previously (27, 28). The degree of cell-cell contact in confluent monolayers of the cells was modulated by adjusting the Ca^{2+} concentration of the growth medium between 5 μM (LC-medium) and 1.8 mM (HC-medium) (for details see references 28, 29).

Preparation of a Desmosome-enriched Fraction from Bovine Muzzle Epidermis

The purification of desmosomes from fresh bovine muzzle epidermis, and the separation of membrane core glycoproteins from cytoplasmic plaque proteins were performed as described previously (15, 31, 36).

Antibodies

The characteristics and specificities of antibodies to DPI/II and DGI have been described previously (31–33). Mouse mAbs specific for human epithelial cytokeratins (AE1:AE3) and β-tubulin were purchased from Boehringer-Mannheim Biochemicals (Indianapolis, IN) and Amersham Corp. (Amersham, UK), respectively.

Metabolic Labeling and Cell Fractionation

Confluent monolayers of MDCK cells were grown at 37°C in DMEM containing 5 μM Ca^{2+} in 10% dialyzed FBS (LC-medium) on collagen-coated 35-mm petri dishes or glass coverslips as described previously (31–33). Cells were labeled metabolically with [^{35}S]methionine (1,200 Ci/mmol; New England Nuclear, Boston, MA) for 10 min at 37°C and then chased for different periods of time in a >10,000-fold excess of unlabeled methionine in LC-medium at 19°C. At the end of the chase period, cells were transferred to 4°C, rinsed twice with Tris-Saline (10 mM Tris-HCl, pH 7.4, 120 mM NaCl) containing 1 mM PMSF, and then extracted in 300 μl of an isotonic buffer containing Triton X-100 (0.5% [vol/vol] Triton X-100, 10 mM Tris-HCl, pH 7.5, 25 mM KCl, 120 mM NaCl, 2 mM EGTA, 2 mM EDTA, 0.1 mM DTT, and 0.5 mM PMSF) for 10 min at 4°C on a rocking platform. The monolayer of cells were scraped from the petri dishes into the extraction buffer and centrifuged for 10 min at 48,000 *g*. The resulting supernatant was layered onto a 3.7-ml linear 5–20% (wt/wt) sucrose gradient in extraction buffer but without Triton X-100, and centrifuged at 486,000 *g* for 5 h at 4°C in the SW60 Ti rotor of the L8-70M ultracentrifuge (Beckman Instruments, Inc., Fullerton, CA). Gradients were fractionated from the bottom to the top into 20 fractions (200 μl each). The following protein standards of known S values were centrifuged on replicate 5–20% (wt/wt) sucrose gradients; apoferritin, 17.2S; catalase 11.35S; aldolase 7.35S; BSA, 4.6S; cytochrome *c*, 1.7S. The distribution of these protein standards in the sucrose gradient was determined by SDS-PAGE followed by staining the gel with Coomassie blue (for details, see reference 27).

Immunoprecipitation

Immunoprecipitations were performed as described previously (31, 33) with the following exception; the final pellet of protein A-Sepharose CL-4B beads containing antigen-antibody complexes was washed twice in low salt concentration buffer containing 10 mM Tris-HCl pH 7.5, 2 mM EDTA, and 5 mM DTT. The resulting pellet was resuspended in 45 μl of SDS sample buffer and processed for SDS 5% PAGE and fluorography as described previously (31, 33).

The relative amount of radioactivity in the protein bands corresponding to DPI/II and DGI was determined from the resulting fluorograms by scanning densitometry using a DU-7 spectrophotometer (Beckman Instruments, Inc.) equipped for automatic integrations; all x-ray films were preflashed (28), and several different exposures were analyzed. The data is expressed as normalized arbitrary units as described previously (31). In each case, data from one typical experiment are presented, although all experiments were performed between three and five times.

Indirect Immunofluorescence

Our previous studies showed that transport of DGI to the plasma membrane can be blocked in the Golgi complex by incubating cells at 19°C for short periods; this block is completely reversible by returning cells to 37°C. (See reference 33 for details.) We have utilized this procedure as a method to synchronize the arrival at the plasma membrane of DGI and DPI/II during induction of desmosome assembly caused by cell-cell contact. MDCK cells were maintained at single cell density for 60–72 h, trypsinized and plated at confluent density in LC-medium on collagen-coated glass coverslips (for details, see references 31–33). Cells were incubated at 37°C for 4–6 h. The LC-medium was replaced with LC-medium containing 4 μg/ml cycloheximide and cells were incubated at 37°C for a further 8 h. The cycloheximide-containing medium was removed. The cells were rinsed in fresh LC-medium and incubated at 19°C for 3 h. The LC-medium was removed and replaced with LC-medium, and the cells were transferred to 37°C for 30 min to 1 d. At each time point, cells were rinsed with PBS and either fixed/permeabilized with 100% methanol at −20°C, or extracted with CSK buffer (see reference 12) and then fixed in a solution of 1.75% formaldehyde in PBS. Cells were then processed for indirect immunofluorescence as described in detail previously (31). For double immunofluorescence, either a mouse mAb to cytokeratin (1:100 dilution in PBS) or β-tubulin (1:300 dilution) was applied together with either of the monospecific rabbit polyclonals

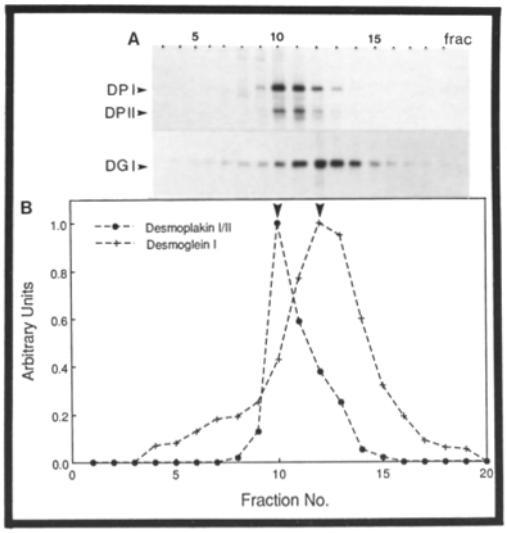

Figure 1. Sedimentation profiles of soluble pools of DGI and DPI/II in sucrose gradients. Confluent monolayers of MDCK cells were established in LC-medium and metabolically labeled with 500 μCi [^{35}S]methionine. Cells were chased in 10,000 fold excess methionine in LC-medium at 19°C for 3 h and then extracted in isotonic buffer containing Triton X-100. Solubilized proteins were fractionated in 5–20% (wt/wt) sucrose gradients in isotonic buffer. Gradients were fractionated (20 fractions; fraction 1 is the bottom of the gradient) and the distributions of proteins were determined by immunoprecipitation with antibodies to DGI or DPI/II, followed by SDS 5% PAGE and autoradiography (*A*). The autoradiograms from immunoprecipitations in *A* were quantified by scanning densitometry (*B*). The values obtained were normalized to the highest values (peak fraction), which was assigned a value of 1.

raised against DPI/II (1/200 dilution) or DGI (1/100 dilution). The mouse antibodies were visualized with FITC-conjugated anti-mouse IgG (Boehringer-Mannheim; 1/100 dilution in PBS). The rabbit antibodies were visualized with rhodamine-conjugated anti-rabbit IgG (Boehringer-Mannhein; 1/100 dilution in PBS). Coverslips were mounted in Elvanol (34) containing 0.2% paraphenylene diamine (pH 8.6) and viewed in a Zeiss axiophot microscope equipped with epifluorescence illumination.

Results

Sedimentation of Soluble Pools of DGI and DPI/II in Sucrose Density Gradients

To obtain soluble pools of newly synthesized DGI and DPI/II, MDCK cells were pulse-labelled with [^{35}S]methionine and then incubated at 19°C to accumulate DGI in the Golgi complex before transfer of the protein to the insoluble pool (for details, see reference 33). Cells were extracted, and solubilized proteins separated in sucrose gradients.

The sedimentation profile of DGI is broad with the majority of protein sedimenting in fractions 10–14, with the peak fraction at fraction 12 (~6.2S) (Fig. 1, *a* and *b*). Analysis of the sedimentation profiles of DPI and II revealed that the proteins cosedimented. The sedimentation profile of DPI/II is less broad than that of DGI with the majority of the proteins sedimenting in fractions 10–12 (peak in fraction 10; ~7.3S) (Fig. 1, *a* and *b*). These results show that the sedimentation profiles of DGI and DPI/II overlap, but that the peak fractions of each protein have distinctly different sedimentation rates.

The Triton X-100–solubilized Pools of DGI and DPI/II Do Not Coimmunoprecipitate

We searched for possible interactions between DGI and DPI/II in sucrose gradient fractions in which the distributions of the proteins overlapped by using immunoprecipitation with specific antibodies. The immunoprecipitations were carried out under low stringency (LS) conditions to preserve possible interactions between DGI and DPI/II (Fig. 2, *c* and *d*, see Materials and Methods). Under these conditions, both DPI and II were coimmunoprecipitated with DPI/II antibodies (Fig. 2, *a* and *c*; also see reference 31); however, DGI was not co-immunoprecipitated with DPI/II. Similarly, when these fractions were immunoprecipitated with DGI antibodies, we detected DGI but neither DPI/II in the immunoprecipitate. The results show that the extracted pools of soluble DGI and DPI/II do not appear to be associated.

Spatial Organization of Membrane Core and Cytoplasmic Plaque Proteins before Induction of Cell–Cell Contact

Previous analyses of desmosomal protein distributions have shown complicated staining patterns in epithelial cells before the assembly of proteins into desmosomes at the plasma membrane (see reference 32). This complexity is the result of asynchrony in the processing and transfer of proteins to the plasma membrane. Under these conditions, the staining patterns of DGI and DPI/II appear different (Fig. 5).

We have sought to develop a method to synchronize transfer of desmosomal proteins to the plasma membrane and desmosomal assembly. We have used a short 19°C temperature block (26) to synchronize these events. Previously, we showed that intracellular processing and transport of DGI to the cell surface is blocked in the Golgi complex in cells

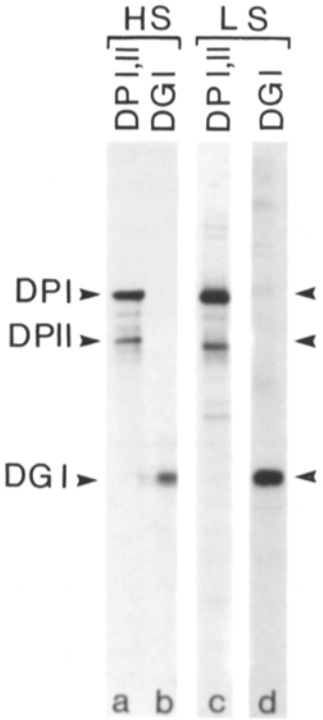

Figure 2. Low stringency immunoprecipitation of DGI and DPI/II from sucrose gradients. The soluble pools of [^{35}S]methionine-labeled DGI and DPI/II were fractionated in sucrose gradients as described in the legend to Fig. 1. Fractions of the sucrose gradient that contained overlapping distributions of DGI and DPI/II (fractions 9–13, see Fig. 1) were pooled and processed for immunoprecipitation with antibodies against either DGI and/or DPI/II. Immunoprecipitations were carried out under high stringency (*HS*; *a* and *b*) or low stringency (*LS*; *c* and *d*) conditions. Arrows indicate the position of DPI, II, and DGI, respectively.

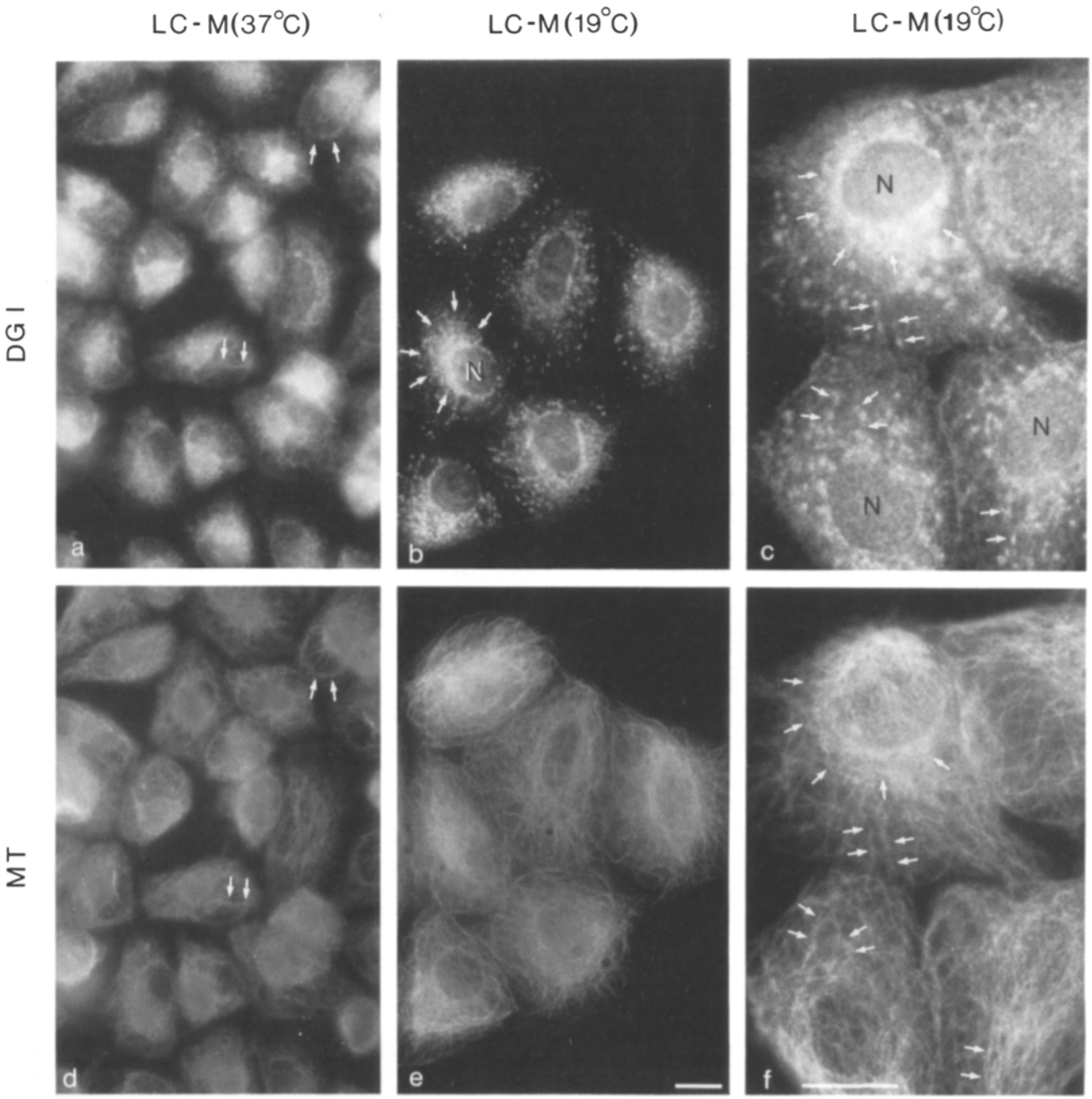

Figure 3. Double indirect immunofluorescence of DGI (*a–c*) and β-tubulin (*d–f*) in MDCK cells maintained at 37°C (*a* and *d*) or 19°C (*b*, *c*, *e*, and *f*). Cultures of MDCK cells were established and maintained at 37°C (*a* and *d*) or transferred to 19°C for 3 h (*b*, *c*, *e*, and *f*). Cells were fixed and permeabilized in 100% methanol at −20°C and then processed for double immunofluorescence with a rabbit polyclonal antibody against DGI (*a–c*) and a mouse monoclonal antibody against β-tubulin (*d* and *f*), the rabbit and mouse antibodies were visualized with rhodamine- and FITC-conjugated secondary antibodies, respectively. Arrows indicate areas of codistribution of DGI and microtubule bundles (*a*, *d*; *c*, *f*); *N*, nucleus; note perinuclear distribution of DGI in cells maintained transiently at 19°C (*b*, *arrows*). Bar, 15 μm.

grown at 19°C (33). This was confirmed by immunofluorescence microscopy. At 19°C, DGI staining is localized to the perinuclear cytoplasm in association with the Golgi complex (Fig. 3, *a–c*; see also reference 33). Little or no staining of the cell periphery is detected.

A comparable analysis of DPI/II staining revealed significant differences between cells incubated at 19°C (Fig. 4, *b* and *c*) and 37°C (Fig. 4 *a*). At 37°C, a punctate staining pattern was observed throughout the cytoplasm as shown previously (32). However, in cells maintained at 19°C, DPI/II staining was localized to the cytoplasm in the center of the cell from which strings of fluorescent dots extended towards the periphery (Fig. 4 *b*). Higher magnification revealed that the perinuclear staining was composed of fluorescent dots similar to those that extended towards the cell periphery (Fig. 4 *c*). Comparison of the distributions of DGI and DPI/II indicates little or no overlap except in the center of the cell. However, at that site DGI staining was localized

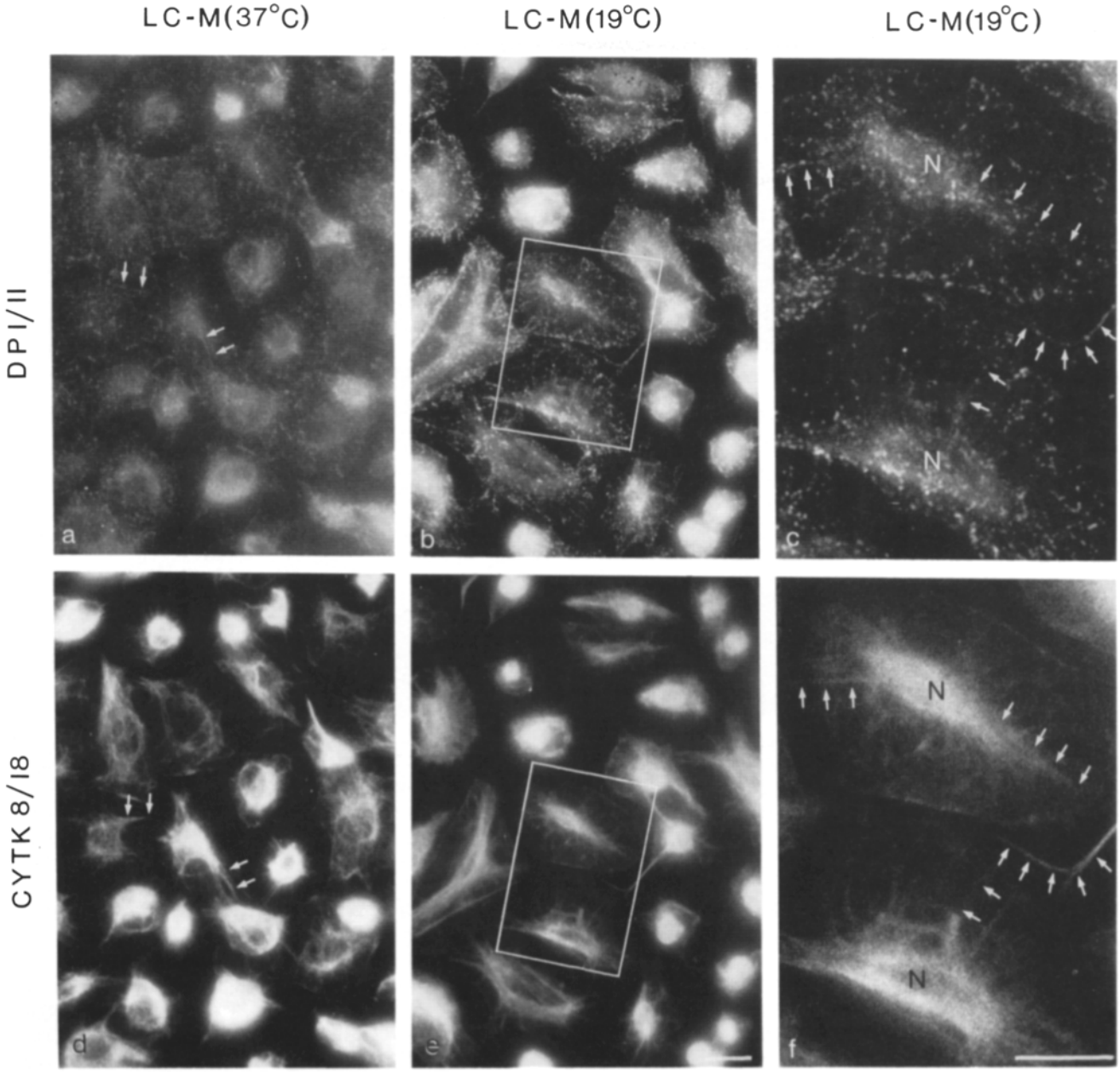

Figure 4. Double indirect immunofluorescence of DPI/II (*a–c*) and cytokeratin intermediate filaments (*d–f*) in MDCK cells maintained at 37°C (*a* and *d*) or 19°C (*b*, *c*, *e*, and *f*) in low Ca^{2+}-medium (LC-M). Cultures of MDCK cells were grown at 37°C or 19°C as described in the legend to Fig. 3. Cells were processed for double immunofluorescence with a rabbit polyclonal antibody against DPI/II (*a–c*) and a mouse monoclonal antibody against cytokeratin intermediate filament proteins 8/18 (Cytk 8/18) (*d–f*). Rabbit and mouse antibodies were visualized with rhodamine and FITC-conjugated secondary antibodies, respectively. Arrows indicate areas of codistribution of cytokeratin intermediate filaments and DPI/II. Boxed areas in *b* and *e* are shown at higher magnification in *c* and *f*, respectively; *N*, nucleus. Bar, 15 μm.

to one side of the nucleus, whereas DPI/II staining appeared over the whole perinuclear space.

Membrane Core and Cytoplasmic Plaque Domains Are Associated with Different Cytoskeletal Elements before Cell–Cell Adhesion

We investigated whether these distinctive distributions of DGI and DPI/II were similar to those of different cytoskeletal filaments. Double indirect immunofluorescence was performed using anti-DGI and anti-β-tubulin antibodies to detect microtubules (Fig. 3). In cells maintained at 37°C DGI exhibited a diffuse, cytoplasmic staining pattern that extended to the cell periphery (Fig. 3 *a*). The staining pattern of microtubules was characterized by bundles of filaments extending throughout the cytoplasm. Close inspection of these cells revealed some overlap in the staining patterns of DGI and β-tubulin (Fig. 3, *a* and *d*). However, analysis of DGI and microtubules in MDCK cells maintained at 19°C revealed an extensive overlap in their distribution. Close inspection of the micrographs reveals discrete patches of DGI staining that line-up along individual bundles of microtubules that radiate from the perinuclear cytoplasm towards the cell periphery (Fig. 3, *b*, *c*, *e*, and *f*). Note that the staining pattern of microtubules was similar in cells grown at ei-

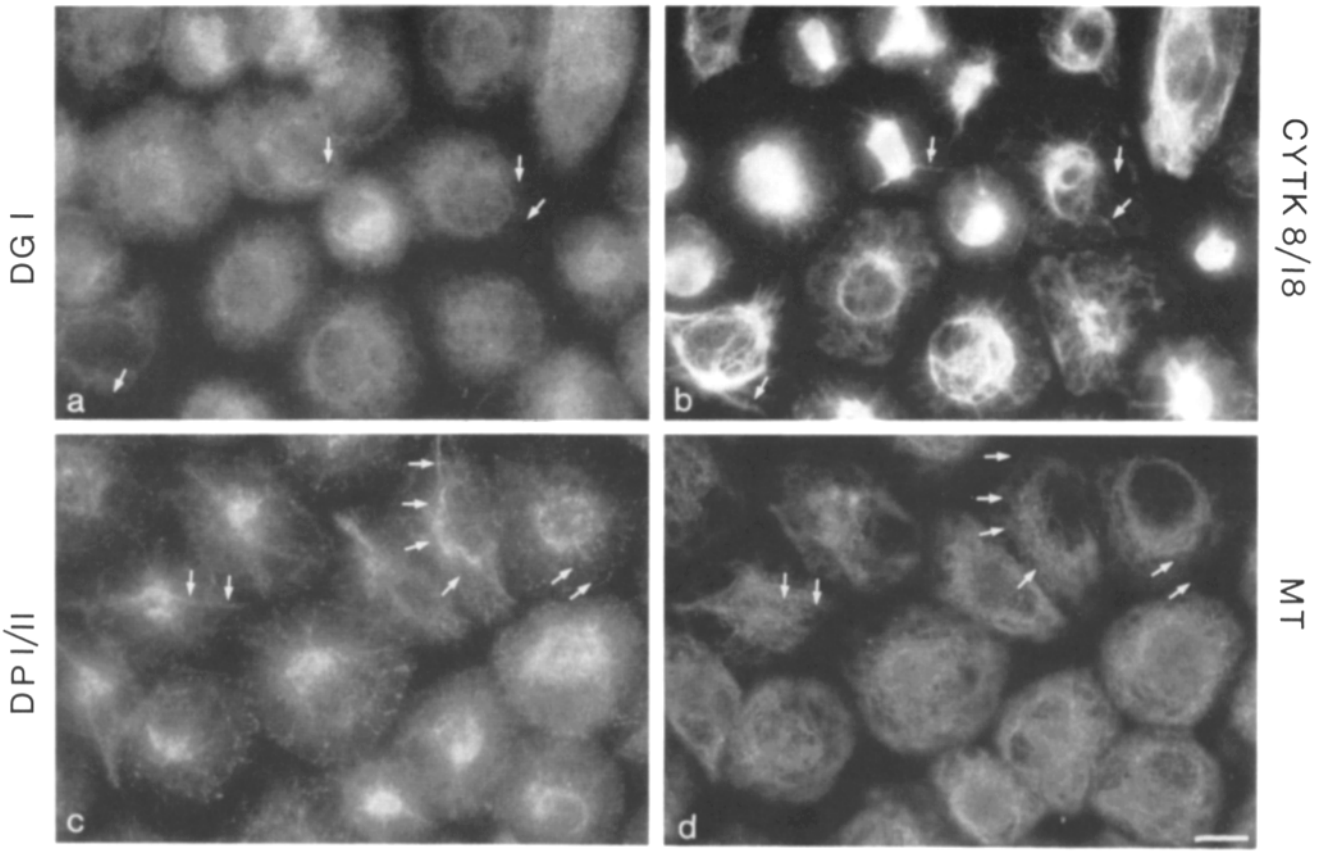

Figure 5. Double indirect immunofluorescence of MDCK cells at 19°C to compare the distributions of DGI and cytokeratin intermediate filaments, and DPI/II and microtubules. Cells were grown at 19°C as described in the legend to Fig. 3 and processed for immunofluorescence with antibodies against DGI (*a*), DPI/II (*c*), cytokeratin protein 8/18 (*b*), and β-tubulin (*d*). Rabbit and mouse antibodies were visualized with rhodamine and FITC-conjugated secondary antibodies. Arrows exemplify regions in which there is little or no overlap of protein distributions. Bar, 15 μm.

ther 37°C or 19°C (Fig. 3, *d* and *e*), indicating that the 19°C block does not affect the subcellular organization of microtubules.

Double immunofluorescence of MDCK cells with anti-DPI/II and a monoclonal antibody against cytokeratin intermediate filaments showed a distinctive overlap in the distribution of these proteins. In cells grown at 37°C, DPI/II exhibited a punctate staining pattern (Fig. 4 *a*) which, in many cases, appeared to be codistributed with the staining pattern of cytokeratin filaments (Fig. 4 *d*). However, codistribution of DPI/II and cytokeratin filaments was clear in cells incubated at 19°C. At 19°C, DPI/II had a distinct, punctate staining pattern comprised of lines of dots, (Fig. 4, *b* and *c*) that are clearly localized along individual bundles of cytokeratin filaments (Fig. 4, *e* and *f*). Note that the cytokeratin filament staining pattern is similar in cells maintained at either 37°C or 19°C, showing that the 19°C block does not affect the subcellular organization of cytokeratin filaments.

We also compared the distribution of DGI and cytokeratin filaments (Fig. 5, *a* and *b*), and DPI/II and tubulin (Fig. 5, *c* and *d*). The staining patterns were different indicating little or no co-distribution of these pairs of proteins, as expected from the comparative analysis of the distribution of DGI and DPI/II (see Fig. 5, *a* and *c*).

Reorganization of Membrane Core and Cytoplasmic Plaque Proteins upon Induction of Cell–Cell Contact

The results described above show different intracellular distributions of components of the membrane core and cytoplasmic plaque in cells grown in the absence of cell–cell contact. We next examined these distributions, together with those of microtubules and cytokeratin filaments, during induction of cell–cell interactions and assembly of desmosomes at the plasma membrane.

As shown earlier, at 19°C the staining pattern of DGI is located in a perinuclear region of the cytoplasm in cells maintained in LC-medium (Fig. 6 *a*). Upon induction of cell–cell contact and transfer to 37°C, DGI staining becomes more homogeneous throughout the cytoplasm and extends towards the cell periphery (Fig. 6, *b* and *c*). Close inspection of the micrographs reveals staining of DGI along bundles of microtubules that extend to the cell periphery. 24 h after induction of cell–cell contact, the majority of the intracellular DGI staining has disappeared, and intense peripheral staining at the areas of cell–cell contact is found (Fig. 6 *d*).

The staining pattern of microtubule filaments also changes during induction of cell–cell contact (Fig. 6, *e–h*). The initial fibrous staining pattern radiating from the perinuclear region is replaced by a more homogenous staining pattern that may

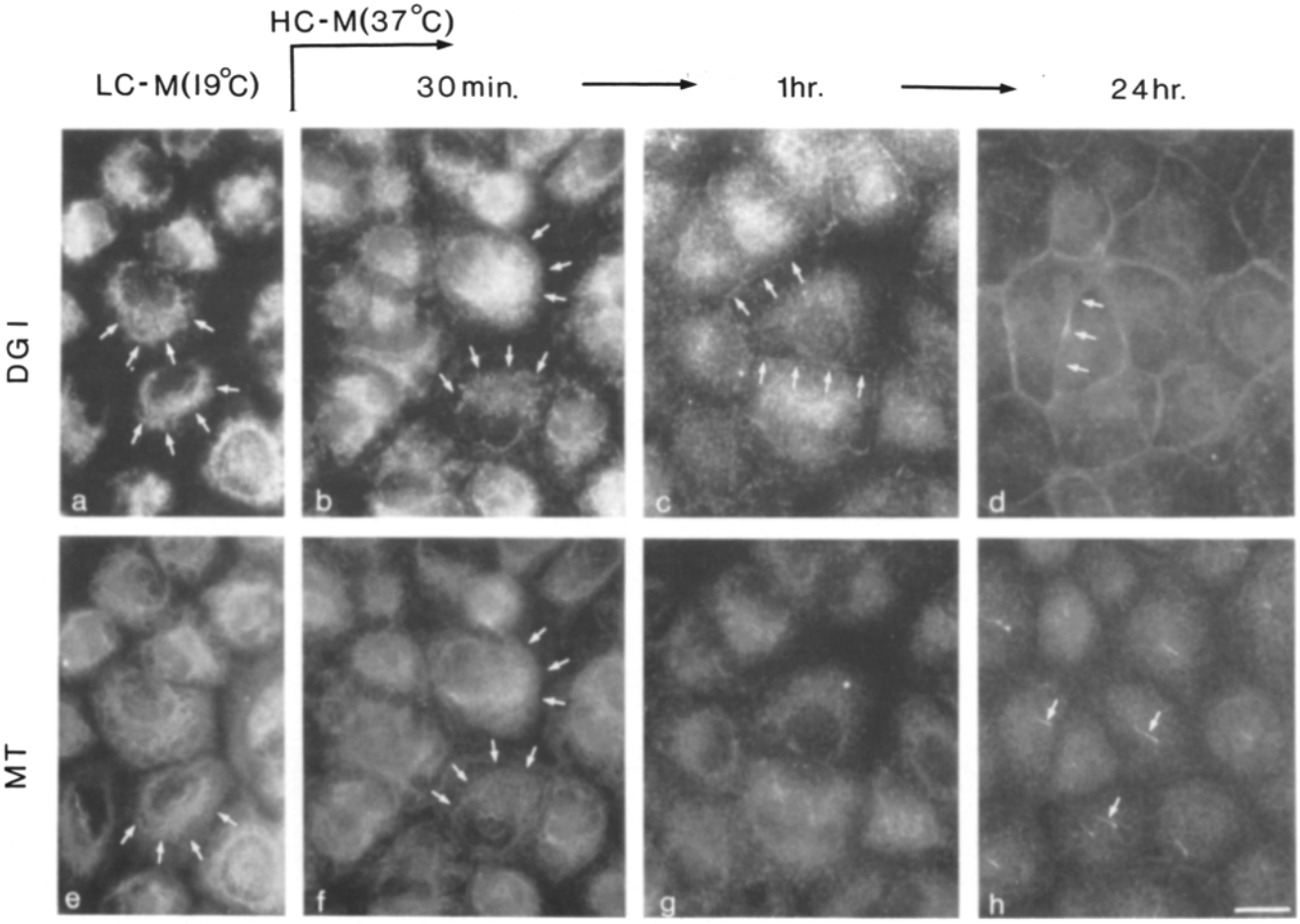

Figure 6. Double indirect immunofluorescence of DGI and β-tubulin in MDCK cells during induction of cell–cell contact at 37°C. Confluent monolayers of MDCK cells were established in LC-medium at 37°C and then incubated at 19°C for 3 h (*a* and *e*). Cell–cell contact was then induced by replacing the LC-medium with HC-medium at 37°C for 30 min (*b* and *f*), 1 h (*c* and *g*) or 24 h (*d* and *h*). Cells were then fixed and permeabilized with methanol at −20°C and processed for double immunofluorescence with rabbit polyclonal antibodies against DGI (*a–d*) and mouse monoclonal antibody against β-tubulin (*e–h*). Rabbit and mouse antibodies were visualized using rhodamine and FITC-conjugated secondary antibodies. Arrows indicate the areas of co-distribution of DGI and microtubule bundles (*a*, *e*; *b*, *f*), the localization of DGI at the plasma membrane upon induction of cell–cell contact (*c* and *d*), and the primary cilium on the apical surface of fully polarized MDCK cells (*h*). Bar, 15 μm.

represent formation of the apical cap of microtubules reported previously in these cells (see reference 4). Note an intensely staining single strand of tubulin at the center of each cell that represents the primary cilium located on the apical surface of fully polarized MDCK cells (see reference 43).

The effects of the cell–cell contact on the subcellular distributions of DPI/II and cytokeratin filaments was also analyzed. As shown above, at 19°C DPI/II staining in cells in LC-medium is punctate and radiates from a more intensely staining perinuclear area to the cell periphery (Fig. 7 *a*). Induction of cell–cell contact and transfer to 37°C results in reorganization of DPI/II. At each time point, the amount of intracellular punctate staining declines rapidly. Concomitantly, there is increased staining of DPI/II at the periphery of the cell in the areas of cell–cell contact (Fig. 7, *b* and *c*). 24 h after induction of cell–cell contact the majority of DPI/II staining is localized to the plasma membrane with little or no intracellular staining (Fig. 7 *d*). The staining pattern of cytokeratin filaments also changes upon induction of cell–cell contact from a densely staining perinuclear location to a staining pattern localized predominantly to the periphery of cells in association with cell–cell contacts and assembled desmosomes (Fig. 7 *e*).

Discussion

Desmosomes are complex, multisubunit structures that comprise at least 8 different cytoplasmic and integral membrane proteins that are organized into two domains, a cytoplasmic plaque and a membrane core. A fundamental issue is to understand the regulation of protein assembly into each of these domains, and how each domain is integrated into a desmosome at the cell surface. An important insight into this problem is that assembly of desmosomes is initiated from preexisting pools of proteins present in the cell before induction of cell–cell contact (20, 21, 31–33). What is the nature of these preexisting pools of desmosomal proteins? At least two possibilities exist: First, domains may be coassembled intracellularly and delivered to the plasma membrane as an integrated half-desmosome complex. Second, each domain

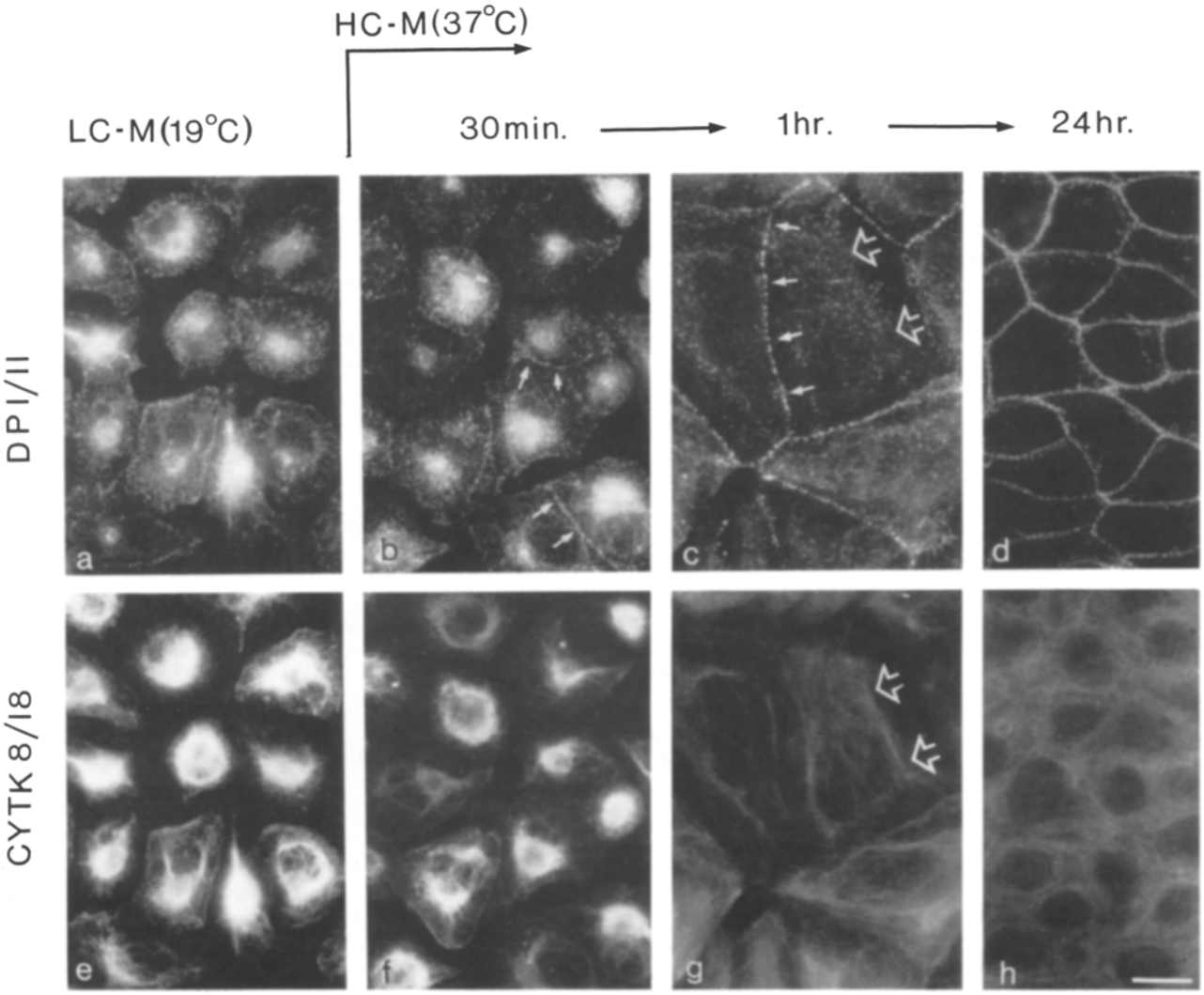

Figure 7. Double indirect immunofluorescence of DPI/II and cytokeratin intermediate filaments during induction of cell–cell contact at 37°C. Cultures of MDCK cells were processed as described in the legend to Fig. 6. Cells were grown at 19°C in LC-medium (*a*, *e*), or subsequently transferred to 37°C in HC-medium for 30 min (*b*, *f*), 1 h (*c*, *g*), or 24 h (*d*, *h*). Cells were then extracted with CSK buffer (see Materials and Methods), fixed in 1.75% formaldehyde and processed for double immunofluorescence with a rabbit polyclonal antibody against DPI/II (*a–d*) and a mouse monoclonal antibody against cytokeratin (*e*, *h*). Rabbit and mouse antibodies were visualized with rhodamine and FITC-conjugated secondary antibodies, respectively. Small arrows (*b*, *c*) indicate the localization of DPI/II at the plasma membrane upon induction of cell-cell contact. Bar, 15 μm.

may be assembled separately within the cell with their integration into a desmosome coordinated at the cell surface.

To distinguish between these possibilities, we compared the intracellular distribution of major components of the cytoplasmic plaque domain (DPI/II) and membrane core domain (DGI). Previously, we showed that upon synthesis these proteins initially enter a pool of protein(s) that is soluble in buffer containing Triton X-100, which is subsequently titrated into a pool of protein(s) that is insoluble in this buffer. Significantly, we showed that both pools of protein occur intracellularly and before desmosome assembly (31, 33). Either of these pools, therefore, represents a site where preassembly and interactions between desmosomal domains could occur. In the present study we searched for interactions between DGI and DPI/II in the soluble pool of proteins by analysis of their sedimentation properties in sucrose gradients. Since the insoluble pool is resistant to extraction from cells except with chaotropic agents, which might disrupt protein complexes, we analyzed the spatial distribution of the insoluble pools of DPI/II and DGI by immunofluorescence; the resolution of this analysis was greatly enhanced by transiently incubating cells at 19°C to synchronize desmosome assembly (see below).

Soluble Pools of Membrane Core and Cytoplasmic Plaque Proteins Are Not Associated

Sucrose density gradient fractionation of the Triton X-100-soluble pools of proteins from MDCK cells demonstrated an overlap in distributions but a significant difference in the peak fractions of DGI (6.2S) and DPI/II (7.3S). Increasing or decreasing the time of centrifugation caused a corre-

sponding shift in the sedimentation profiles of both proteins, indicating that these distributions are not the result of an equilibrium centrifugation. It is possible that the buffer conditions used for extraction and fractionation of proteins caused dissociation of a complex of these proteins. However, the complex of DPI and II was retained after detergent extraction and sucrose gradient fractionation under these conditions. Also, it is noteworthy that under these conditions interactions between integral membrane proteins and cytoplasmic proteins are retained. For example, we previously demonstrated that protein complexes making up Na^+, K^+-ATPase, ankyrin and fodrin are retained under these conditions (27).

We sought a second criterion for testing the association of DPI/II and DGI in the soluble pool by direct immunoprecipitation of proteins under low stringency conditions in which protein-protein interactions are normally retained. Immunoprecipitation of proteins from sucrose gradient fractions in which the sedimentation profiles of DPI/II and DGI overlapped, demonstrated that DGI and DPI/II were not coimmunoprecipitated either with DGI or DPI/II-specific antibodies (Fig. 2, *a–d*). Under the same immunoprecipitation conditions, the interaction between DPI and II was maintained (Fig. 2, *a* and *c*). Together, these biochemical data indicate that within the pool of proteins solubilized in Triton X-100, DGI and DPI/II do not appear to be associated in a protein complex.

Different Spatial Distributions of Membrane Core and Cytoplasmic Plaque Proteins before Desmosome Assembly

The spatial distributions of membrane core (DGI) and cytoplasmic plaque domains (DPI/II) were investigated by immunofluorescence of MDCK cells before induction of cell–cell contacts. At 37°C, the staining patterns of DGI and DPI/II were diffuse throughout the cytoplasm and extended from the cell center to the periphery. Interpretation of these patterns is complex (31–33) due to the fact that proteins are present in both soluble and insoluble pools, and that, in the case of DGI, proteins are located at different intracellular organelles involved in posttranslational processing of membrane proteins (i.e., between the ER, Golgi complex, and plasma membrane).

To better resolve the distributions of these proteins as a function of stages in desmosome assembly, we used a 19°C temperature block (26) to synchronize desmosomal protein processing and assembly. Previously, we showed that DGI processing and transport to the plasma membrane is blocked in cells grown for short periods at 19°C (see reference 33). Under these conditions, newly synthesized DGI remains sensitive to digestion with Endo H and is extracted from cells in buffers containing Triton X-100; these characteristics indicate that the block in DGI processing is in the early Golgi complex (for details see reference 33). Significantly, upon raising the incubation temperature of these cells to 37°C, we showed that complex glycosylation of DGI is rapidly completed and the protein enters an insoluble pool. DGI is subsequently transported from the Golgi complex to the cell surface with kinetics similar to those of DGI in cells maintained continuously at 37°C. Thus, the 19°C block in DGI transport is transient and completely reversible.

The 19°C block in DGI processing has an advantage for the present study since it results in the differential accumulation of DGI in the Golgi complex. Previously, we showed that cell surface DGI is rapidly degraded ($t_{1/2}$ ~2 h) in cells grown in the absence of cell–cell contacts. Hence, over a short time period at 19°C the cell surface pool of protein is rapidly degraded and DGI staining increases in the perinuclear cytoplasm as newly synthesized protein accumulates in the Golgi complex (Fig. 3, *b* and *c*). A comparable analysis of DPI/II distributions in cells incubated transiently at 19°C showed staining in ordered arrays extending from the center of the cell to the periphery. This distribution of DPI/II is significantly different from that of DGI. Within the cytoplasm and at the cell periphery we observed little or no evidence of colocalization of DGI and DPI/II.

Upon raising the incubation temperature of cells to 37°C and inducing cell–cell contact by increasing extracellular Ca^{2+} concentration, there was a rapid clearing of DGI and DPI/II staining from the center of each cell, and a concomitant appearance of staining at the areas of cell–cell contact. Within 1–3 h after induction of cell–cell contact, the staining patterns of DGI and DPI/II at the plasma membrane are indistinguishable, corresponding to the assembly of these proteins into individual desmosomes. These results demonstrate that the block in desmosomal protein processing and assembly is completely reversible, and that DGI and DPI/II rapidly coassemble at the plasma membrane upon induction of cell–cell contact.

A recent study by Duden and Franke (9) raised the possibility that the insoluble pool of DPI/II in single cells represents protein from previous desmosomes that was internalized after loss of cell–cell contact and then persisted in the cytoplasm. To avoid this problem, we have precultured the MDCK cells used for these types of experiments at very low density for up to 72 h. Under these conditions, we have found that DPI/II present before the preculture step are rapidly degraded in the absence of extensive cell–cell contact ($t_{1/2}$ ~8 h); over a 72 h period, this rate of turnover results in <0.02% of the original DPI/II remaining in the cell at the time they are plated at confluent density of LC-medium. Also, it is noteworthy that upon induction of cell–cell contacts, the distinctive cytoplasmic arrays of insoluble DPI/II are rapidly cleared from the cytoplasm. Concommitantly, a punctate DPI/II staining appears at the cell surface in the areas of cell–cell contact, indicating a distinct recruitment of the cytoplasmic pool of DPI/II to the forming desmosomes on the plasma membrane.

Membrane Core and Cytoplasmic Domains Are Associated with Different Cytoskeletal Elements

The staining pattern of DPI/II in cells transiently incubated at 19°C appeared highly organized in linear arrays. Previous studies by us and other investigators have indicated an association between cytokeratin intermediate filaments and DPI/II (20, 21, 32). The colocalization at these proteins is very distinct in cells incubated at 19°C. The cytokeratin staining was localized in an intense perinuclear aggregate from which bundles of filaments radiated towards the cell periphery. DPI/II were also localized in the perinuclear cytoplasm, but also prominently as strings of fluorescent dots that extended towards the periphery of the cell. The staining

pattern of DPI/II was distinct from that of microtubules (Fig. 5, *c* and *d*) and microfilaments (data not shown).

A comparable analysis of the subcellular distributions of DGI and tubulin showed that the perinuclear punctate staining of DGI was colocalized with bundles of microtubules emanating from the perinuclear region and Golgi complex (Fig. 3, *c* and *e*, and *d* and *f*). That DGI and microtubules may be associated is not surprising. Recent studies have demonstrated roles of microtubules in vesicular transport and in the organization and maintenance of integrity of the Golgi complex (39). In addition, mechanochemical proteins, such as kinesin and dynein, have been shown to be involved in movement of vesicles along microtubules (40).

Mechanisms of Intracellular Assembly and Organization of Desmosomal Domains

We propose that different cytoskeletal elements regulate the subcellular organization and assembly of desmosomal domains at the plasma membrane. For the membrane core protein DGI, transport in vesicles to the plasma membrane may be facilitated by tracks of microtubules from the Golgi complex to the cell periphery. Our study showed that after induction of cell contact in cells in which desmosome assembly was synchronized, the distribution of DGI spread from the immediate vicinity of the Golgi complex to the cell periphery in conjunction with the microtubule distribution. Although we do not know how vesicles containing DGI, and possibly other membrane core proteins move along microtubules, it is possible that mechanochemical proteins such as kinesin are involved (40).

The apparent association of DPI/II with cytokeratin filaments implies a role for these filaments in the organization and delivery of the cytoplasmic plaque to sites of desmosome assembly at the plasma membrane. However, unlike microtubules and microfilaments, there is at present no evidence that intermediate filaments can actively translocate proteins or vesicles. Alternatively, DPI/II may move passively towards the cell periphery attached to growing cytokeratin filaments. Several studies have identified a nucleation site(s) for intermediate filament assembly in the perinuclear cytoplasm from which intermediate filaments emanate towards the cell periphery (1, 2). If DPI/II complexes attached to filaments randomly in the cytoplasm they could be translocated to the cell periphery as the filament(s) grow by addition of new subunits at the nucleation site.

How is the assembly of membrane core and cytoplasmic plaque coordinated at the plasma membrane? It is possible that membrane core proteins delivered to sites of cell–cell contact may act as a nucleation site for assembly of DPI/II and other cytoplasmic plaque proteins; as the latter arrive at the plasma membrane attached to growing cytokeratin filaments (see above), they may anchor the cytokeratin network to the desmosome forming an interlinking structural matrix between the cytoplasm and plasma membrane. These roles for cytoskeletal filaments should be amenable to experimental test by disrupting individual filament systems and analyzing the effects on membrane core and cytoplasmic plaque domain assembly.

This work was supported in part by grants to W. J. Nelson from the National Institute of Health (GM-35527), The National Science Foundation (DIR 881143X), and the American Heart Association (Grants-in-Aid). W. J. Nelson is a recipient of an Established Investigator Award from The American Heart Association.

Received for publication 28 September 1990 and in revised form 31 January 1991.

References

1. Albers, K., and E. Fuchs. 1987. The expression of mutant epidermal keratin cDNAs transfected in simple epithelial and squamous cell carcinoma lines. *J. Cell Biol.* 105:791–806.
2. Albers, K., and E. Fuchs. 1989. Expression of mutant keratin cDNAs in epithelial cells reveals possible mechanisms for initiation and assembly of intermediate filaments. *J. Cell Biol.* 108:1477–1493.
3. Arnn, J., and L. A. Staehelin. 1981. The structure and function of spot desmosomes. *Dermatology.* 20:330–339.
4. Bacallao, R., C. Antony, C. Dotti, E. Karsenti, E. H. Stelzer, and K. Simons. 1989. The subcellular organization of Madin-Darby Canine Kidney cells during formation of a Polarized epithelium. *J. Cell Biol.* 109:2817–2832.
5. Ball, R. H., and S. J. Singer. 1981. Association of microtubule and intermediate filaments in normal fibroblasts and its disruption upon transformation by temperature sensitive mutant of Rous sarcoma virus. *Proc. Natl. Acad. Sci. USA.* 78:6986–90.
6. Campbell, R. D., and J. H. Campbell. 1971. Origin and continuity of desmosomes. *In* Origin and Continuity of Cell Organelles. J. Reinert and H. Ursprung, editors. Springer-Verlag, Berlin/Heidelberg/New York. 261–298.
7. Cowin, P., and D. R. Garrod. 1983. Antibodies to epithelial desmosomes show wide tissue and species cross reactivity. *Nature (Lond.).* 302: 148–150.
8. Cowin, P., D. L. Mattey, and D. R. Garrod. 1984. Identification of desmosomal surface components (desmocollins) and inhibition of desmosome formation by specific Fab. *J. Cell Sci.* 70:41–60.
9. Duden, R., and W. W. Franke. 1988. Organization of desmosomal plaque proteins in cells growing at low calcium concentrations. *J. Cell Biol.* 107:1049–1063.
10. Edelman, G. M. 1985. Cell adhesion and molecular processes of morphogenesis. *Annu. Rev. Biochem.* 54:135–169.
11. Farquhar, M. G., and G. E. Palade. 1963. Junctional complexes in various epithelia. *J. Cell Biol.* 17:375–412.
12. Fey, E. G., K. M. Wan, and S. Penman. 1984. Epithelial cytoskeletal framework and nuclear matrix-intermediate filament scaffold: three-dimensional organization and protein composition. *J. Cell Biol.* 98: 1973–1984.
13. Garrod, D. R., and P. Cowin. 1986. Desmosomes structure and function. *In* Receptors in Tumor Biology. C. M. Chadwick, editor. Cambridge University Press, Cambridge, UK. 95–130.
14. Geiger, B., Z. Avnur, T. Volburg, and T. Volk. 1985. Molecular domains of adherens junctions. *In* The Cell in Contact. G. M. Edelman and J. P. Thiery, editors. John Wiley & Sons, Inc., New York. 461–489.
15. Gorbsky, G., and M. S. Steinberg. 1981. Isolation of intercellular glycoproteins of desmosomes. *J. Cell Biol.* 90:243–248.
16. Gumbiner, B., and K. Simons. 1986. A functional assay for proteins involved in establishing an epithelial occluding barrier: identification of a uvomorulin-like polypeptide. *J. Cell Biol.* 102:457–468.
17. Gumbiner, B., B. Stevenson, and A. Grimaldi. 1988. The role of the cell adhesion molecule uvomorulin in the formation and maintenance of the epithelial junctional complex. *J. Cell Biol.* 107:1575–1587.
18. Guthrie, S. C., and N. B. Gilula. 1989. Gap junctional communication and development. *Trends Neurol. Sci.* 12:12–16.
19. Hynes, R. O., and A. T. Destree. 1978. 10 nm filaments in normal and transformed cells. *Cell.* 13:151–163.
20. Jones, J. C. R., and R. D. Goldman. 1985. Intermediate filaments and initiation of desmosome assembly. *J. Cell Biol.* 101:506–517.
21. Jones, J. C. R., and A. E. Goldman, P. M. Steinert, S. Yuspa, and R. D. Goldman. 1982. Dynamic aspects of the supramolecular organization of intermediate filaments network in cultured epidermal cells. *Cell Motil.* 2:197–213.
22. Kelly, D. E. 1966. Fine structure of desmosome, hemi-desmosomes and an adepidermal globular layer in developing newt epidermis. *J. Cell Biol.* 28:51–72.
23. Kelly, D. E., and F. L. Shienvold. 1976. The desmosome: fine structure studies with freeze-fracture replication and tannic acid staining of sectioned epidermis. *Cell Tissue Res.* 172:309–323.
24. Madara, J. L. 1988. Tight junction dynamics: Is paracellular transport regulated? *Cell.* 53:497–498.
25. Madin, S. J., and N. B. Darby. 1979. American Type Culture Collection Catalogue of Strains II. 30.
26. Matlin, K. S., and K. Simons. 1983. Reduced temperature prevents transfer of a membrane glycoprotein to the cell surface but does not prevent terminal glycosylation. *Cell.* 34:233–243.
27. Nelson, W. J., and R. W. Hammerton. 1989. A membrane cytoskeletal

complex containing Na^+,K^+-ATPase, Ankyrin, and Fodrin in Madin Darby Canine Kidney (MDCK) cells: implications for the biogenesis of epithelial cell polarity. *J. Cell Biol.* 108:893–902.
28. Nelson, W. J., and P. J. Veshnock. 1986. Dynamics of membrane-skeleton (fodrin) organization during development of polarity in Madin-Darby kidney epithelial cells. *J. Cell Biol.* 103:1751–1765.
29. Nelson, W. J., and P. J. Veshnock. 1987. Modulation of membrane-skeleton (fodrin) stability by cell-cell contact in Madin-Darby Canine Kidney epithelial cells. *J. Cell Biol.* 104:1527–1537.
30. Overton, J. 1962. Desmosome development in normal and reassociating cells of early chick blastoderm. *Dev. Biol.* 4:532–548.
31. Pasdar, M., and W. J. Nelson. 1988. Kinetics of desmosome assembly in Madin Darby canine kidney epithelial cells: temporal and spatial regulation of desmoplakin organization and stabilization upon cell-cell contact. I. Biochemical analysis. *J. Cell Biol.* 106:677–685.
32. Pasdar, M., and W. J. Nelson. 1988. Kinetics of desmosome assembly in Madin Darby Canine Kidney epithelial cells: temporal and spatial regulation of desmoplakin organization and stabilization upon cell–cell contact. II. Morphological analysis. *J. Cell Biol.* 106:687–695.
33. Pasdar, M., and W. J. Nelson. 1989. Regulation of desmosome assembly in epithelial cells: Kinetics of synthesis, transport, and stabilization of desmoglein I, a major protein of the membrane core domain. *J. Cell Biol.* 109:163–177.
34. Rodriquez, J., and F. Deinhardt. 1960. Preparation of semipermanent mounting for fluorescent antibody studies. *Virology.* 12:316–317.
35. Sheetz, M. P., and J. A. Spudich. 1983. Movement of myosin-coated fluorescent beads on actin cables *in vitro*. *Nature (Lond.).* 303:31–35.
36. Skerrow, C. J., I. Hunter, and D. Skerrow. 1987. Dissection of the bovine epidermal desmosome into cytoplasmic protein and membrane glycoprotein. *J. Cell Sci.* 87:411–421.
37. Stevenson, B. R., J. M. Anderson, and S. Bullivant. 1988. The epithelial tight junction: structure, function and preliminary biochemical characterization. *Mol. Cell. Biochem.* 83:129–145.
38. Takeichi, M. 1988. The cadherins: Cell–cell adhesion molecules controlling animal morphogenesis. *Development.* 102:639–655.
39. Trinkaus, J. P. 1984. The Forces That Shape the Embryo. *In* Cells into Organs. Prentice-Hall Press, New York.
40. Vale, R. 1987. Intracellular transport using microtubules-based motors. *Annu. Rev. Cell Biol.* 3:347–378.
41. Volk, T., and B. Geiger. 1984. A 135-kd membrane protein of intercellular adherens junctions. *EMBO (Eur. Mol. Biol. Organ.) J.* 3:2249–2260.
42. Wang, E., and R. D. Goldman. 1978. Functions of cytoplasmic fibers in intracellular movements in BHK-21 cells. *J. Cell Biol.* 79:708–726.
43. Wang, A. Z., G. K. Ojakian, and W. J. Nelson. 1990. Steps in the morphogenesis of a polarized epithelium. I. Uncoupling the roles of cell-cell and cell-substratum contact in establishing plasma membrane polarity in multicellular epithelial (MDCK) cysts. *J. Cell Sci.* 95:137–151.